

NONLINEAR FINITE ELEMENT ANALYSIS OF REINFORCED CONCRETE SLABS UNDER IMPACT LOADS

التحليل اللاخطي بطريقة العناصر المحددة للبلاطات الخرسانية المسلحة تحت الاحمال الصدمية

Dr. Adnan Falih Ali

Prof.

Dr. Ali Ghanim Abbas AL-Khafaji

Lecturer

Univ. of Baghdad/ Eng. College/Civil Eng. Dept. Univ. of Kerbala/ Eng. College/Civil Eng. Dept.

Email: ali_altohmazy44@yahoo.com

Mobile:07813611077

ABSTRACT :

This study presents the theoretical study of the nonlinear behavior of reinforced concrete slabs subjected to impact loads .

The nonlinear finite element analysis adopted by ANSYS software were used in this study. Concrete was simulated by eight-node isoparametric brick elements (SOLID 65) since this element is capable to model cracking and crushing of concrete while steel reinforcing bars were modeled by a three dimensional spar element (LINK 8) which has two nodes with three degrees of freedom identical to those of the (SOLID 65).

The effect of reinforcement ratio, dimensions of slabs and support conditions of the slab were studied too. In dynamic analysis, load-time history , deflection-time relation , and stress-time relation were investigated. Crack patterns were also explained. The central deflections of the slabs under impact were found to become smaller as the tensile reinforcing steel ratio increases, but the rate of the decreases in the deflection is less for high steel reinforcement ratio (1.77 %). Also, those deflections were found to be oscillatory in nature but not in-phase with the applied load. However clamping edges of the slabs results in larger oscillation frequencies as compared to the case of simple supports.

Finally , this study showed that, the maximum central deflection of the slabs becomes larger by (20 – 45 %) as the span of the slab increases by (60 – 125 %) .

الخلاصة:

يتناول هذا البحث دراسة نظرية لسلوك البلاطات الخرسانية المسلحة تحت الاحمال الصدمية. تم إجراء التحليل اللاخطي باستخدام طريقة العناصر المحددة وبالاعتماد على برنامج الحاسوب (ANSYS 9.0) في هذه الدراسة. تم استخدام العناصر الطابوقية ذات الثمان عُقد (Solid 65) لتمثيل الخرسانة لان هذا العنصر له القابلية على تمثيل التصدع والسحق في الخرسانة ، بينما مُثل حديد التسليح بعنصر سارية ثلاثي الأبعاد (Link 8) ذو عقدتان في كل منها ثلاثة درجات حرية مماثلة لتلك الموجودة في العنصر (Solid 65) .

تناولت هذه الدراسة ايضا تأثير أبعاد البلاطات، نسبة التسليح، وحالة المساند للبلاطة. في التحليل الديناميكي تم الحصول على علاقة القوة مع الزمن وعلاقة الانحراف مع الزمن وعلاقة الإجهاد في حديد التسليح مع الزمن وكذلك وُضحت أنماط التشقق . وُجد بأن الانحرافات المركزية للبلاطات المفحوصة تحت الاحمال الصدمية تكون اصغر عند زيادة نسبة حديد التسليح ولكن معدل النقصان في الانحرافات يكون اقل لنسبة حديد التسليح العالية (1,77 %) . ايضا وُجد بأن علاقة هذه الانحرافات مع الزمن تكون بشكل متذبذب (oscillatory) ولكن ليس في نفس الطور مع الحمل المسلط . على أي حال فإنه تثبيت حافات البلاطة (clamped supports) يؤدي إلى تذبذب أكبر (more oscillation) بالمقارنة مع حالة المساند البسيطة (simple supports). واخيرا هذه الدراسة اظهرت بان الانحرافات المركزية القصوى للبلاطات تكون اكبر بنسبة (20-40 %) عند زيادة فضاء البلاطة بنسبة (60-125 %) .

Keywords: impact loading , finite element , reinforced concrete , slabs

1. Introduction :

In recent years ,civil engineers have recognized the important effect of dynamic loading on reinforced concrete structures. Dynamic loads may be created from impact of ballistic tornado, impact of projectile missiles ,wind gusts , machine vibrations , moving vehicles ,blast loads , earthquakes , etc.

Impact loading is recognized as the load resulting from collision between two bodies during a very small interval of time . The impact load applied to a structure depends on the striker velocity, the structure and the striker masses, the resulting deformations and the material properties of both bodies[1].

The finite element method has become a powerful tool for the numerical solutions of reinforced concrete structures due to its efficiency when appropriate models are adopted . It has its own flexibility to tackle different problems as compared to other methods . Adopting this method in a computer program provides time saving and reasonable accuracy for designers and researchers dealing with wide range of problems in different aspects.

In this study , nonlinear finite element analysis was used to obtain precise results on the structural behavior of concrete slabs under impact loads.

2. Impact loading

The structural dynamic response of structures subjected to impact loads can be determined if the impact force –time history is known. Therefore the main purpose of the impact analysis is to determine the impact force –time history.

The impact load applied to a structure depends on the mass, velocity and material properties of the impacting body in addition to the mass and material properties of the structure. Therefore , a load-time history of the impact load can be expected. Numerical and analytical studies have been concerned in computing the load-time relation for the impact load and comparing with test results [2,3]. In some studies and codes, a load time-history is suggested for special cases such as the impact load resulting from the impact of an air plane with important structures such as a nuclear power plant [4] as shown in Fig.(1).

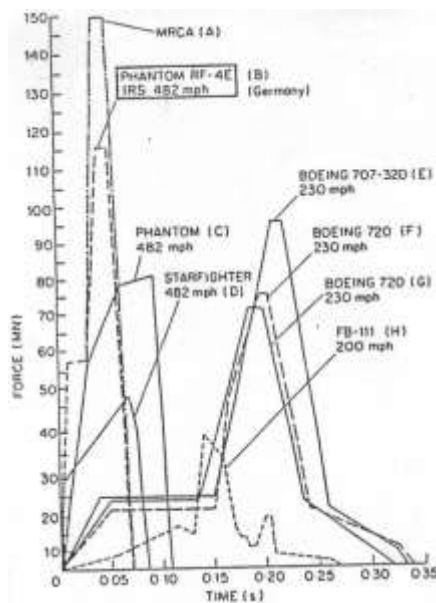


Fig. (1) : Load – time function induced by different types of airplanes [4]

The impact of a rigid spherical striker of a mass (m_{st}) with impact velocity (v_o) applied at the midspan of a slab is shown in Fig. (2). Hertz contact law may be used to relate the force and deformation impact zone , by the following equation :-

$$F(t)=K. [a(t)]^{3/2} \quad \dots\dots(1)$$

where :

$F(t)$: is the impact force at any time (t) within the duration of impact .

$a(t)$: is the deformation at the impact zone at time (t).

K : is the deformation constant which depends on the elastic and geometrical properties of the two bodies .

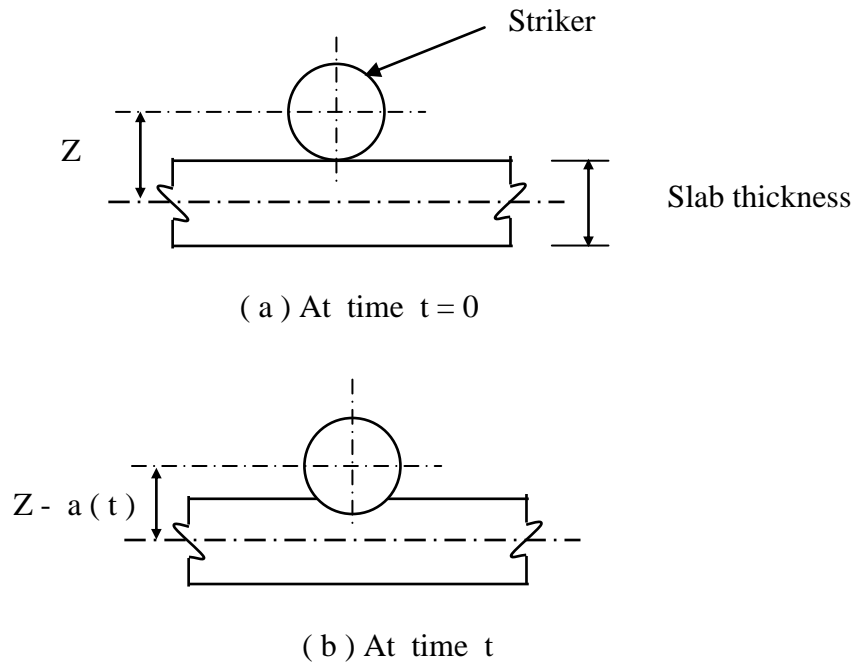


Fig. (2) : Impact of a rigid striker on a slab

The deformation , $a(t)$, at the impact zone is defined as the decrease in distance between the center of gravity of the striker and the slab axis, Fig.(2) .

The deformation equation is :

$$a(t)=Y_s(t) - Y_p(t) \quad \dots\dots(2)$$

where :

$Y_p(t)$: is the slab displacement .

$Y_s(t)$: is the displacement of the rigid striker , and is given by the following equation [1]:

$$Y_s(t)=V_o.t - \frac{1}{m_s} \int_0^t \int_0^\tau F(\bar{\tau}) d\bar{\tau} \quad \dots\dots(3)$$

where m_s and V_o denote the mass and velocity of the striker, respectively .

Substituting equation (3) into (2) , yield :

$$a(t)=V_o.t - \frac{1}{m_s} \int_0^t \int_0^\tau F(\bar{\tau}) d\bar{\tau} - Y_p(t) \quad \dots\dots(4)$$

Thus, equation (1) can be written by the following form :

$$\left(\frac{F(t)}{K}\right)^{2/3} = V_o \cdot t - \frac{1}{m_s} \int_0^t \int_0^\tau F(\bar{\tau}) d\bar{\tau} - Y_p(t) \quad \dots\dots(5)$$

Equation (5) can be solved to give impact force-time history , by using numerical integration method described by Hughes [1] for beams , and Al-Azawi [5] for slabs .

It had been confirmed that the deformation constant (K) depends on the impact velocity [1], therefore the dynamic tests should be carried out to study the effect of impact velocity . Since the special equipment of dynamic test is not available , the deformation constant may be selected so that if satisfied the experimental load-time relationships obtained from the previous experimental dynamic studies , as shown in Fig.(3) .

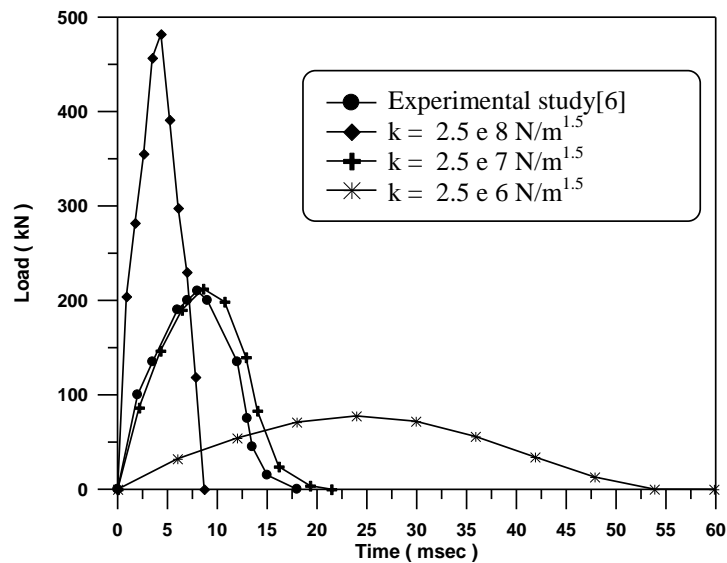


Fig. (3) : Load-time curve for reinforced concrete plate that tested by Murtiadi [6]

Fig. (3) shows the experimental load-time relationship for reinforced concrete plate tested by Murtiadi in Canada in 1999 [6]. In that test , the researcher used plate with dimensions of 950 × 950 × 100 mm and reinforcement ratio (0.95 %) . A rigid projectile was used in that test to apply the impact load to the tested plate. The rigid projectile was a solid steel cylinder with (220 kg) mass and 304.5 mm diameter . The projectile was dropped from a height of (1.5 m) .

Moreover, Fig. (3) shows the theoretical load-time relationships that was performed in the present study by using a computer program described by Al-Khafaji[7]. From this Figure ,it can be noticed that when the deformation constant equals to (2.5e7 N/m^{1.5}) , the theoretical load-time curve approaches greatly the form of the experimental curve , therefore this value for the deformation constant is used in the present study .

3. FINITE ELEMENT ANALYSIS:

The nonlinear finite element analysis is performed using ANSYS software (Version 9.0). The status transition of concrete from uncracked to cracked state and the nonlinear material properties of concrete in compression and steel as it yields cause the nonlinear behavior of the structures under loading. Newton-Raphson equilibrium iteration is used to solve nonlinear problem in ANSYS software. The displacement convergence criterion is used to monitor equilibrium.

3.1. MATERIAL MODELING:

3.1.1. Concrete:

The SOLID 65 , three-dimensional (3D) reinforced concrete solid element , is used to represent concrete in the models . The element , with(2 x 2 x 2) set of Gaussian integration points , is defined by eight nodes having three translational degrees of freedom at each node . This element is capable of cracking in tension and crushing in compression [10] .The most important aspect of this element is the treatment of nonlinear material properties .A schematic of the element is shown in Fig.(4).

The ANSYS program requires the uniaxial stress-strain relation for concrete in compression. Equations (6) and (7) (Desayi and Krishnan 1964 [11]), were used along with Equation (8) to construct the uniaxial compressive stress-strain curve for concrete in this study.

$$f = \frac{E_c \varepsilon}{1 + \left(\frac{\varepsilon}{\varepsilon_o}\right)^2} \dots\dots (6)$$

$$\varepsilon_o = \frac{2f'_c}{E_c} \dots\dots(7)$$

$$E_c = \frac{f}{\varepsilon} \dots\dots(8)$$

where:

f = stress at any strain (ε), MPa .

ε = strain at stress (f)

ε_o = strain at the ultimate compressive strength (f_c')

E_c = The modulus of elasticity of the concrete (MPa) , and was calculated from the following equation :

$$E_c = 4730 \sqrt{f'_c} \dots\dots (9)$$

Fig.(5) shows the simplified compressive uniaxial stress-strain relationship that was used in this study.

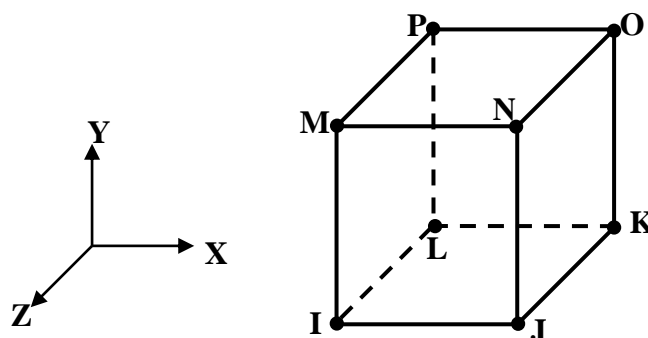


Fig. (4) : SOLID 65 [10]

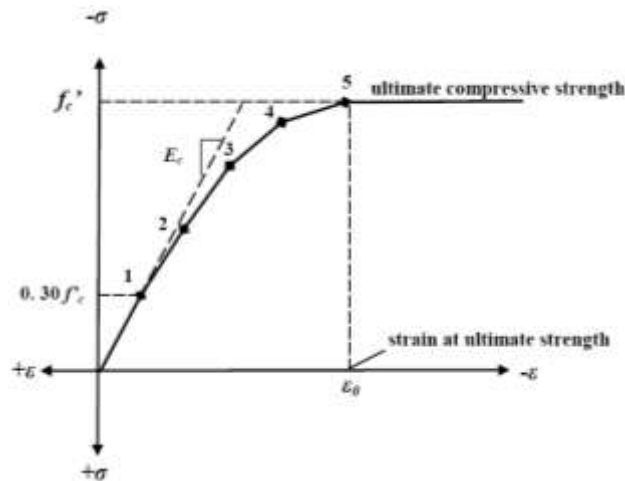


Fig. (5): Simplified compressive uniaxial stress-strain curve for concrete [12]

3.1.2. Reinforcing Steel :

Steel reinforcement is modeled using a discrete model .The reinforcement in this model uses bar elements that are connected to the concrete mesh , therefore , the concrete and the reinforcement mesh share the same nodes , as shown in Fig.(6) .

The Link8 , 3-D spar element is used to model steel reinforcement. Two nodes are required for the Link8 element. At each node, degrees of freedom are identical to those for the SOLID65 element[10] .This element is shown in Fig.(7).

The steel is assumed to be an elastic – perfectly plastic material and identical in tension and compression ,as shown in Fig.(8) .

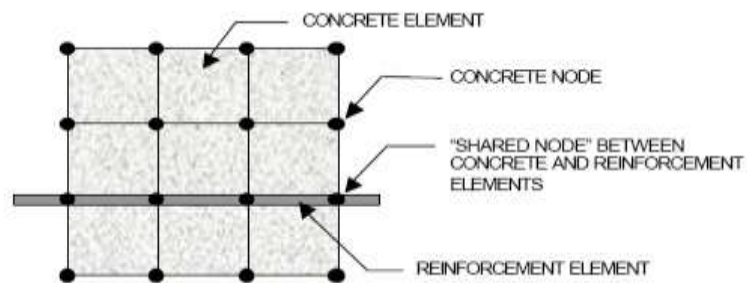


Fig.(6) : Discrete model for reinforcement in reinforced concrete

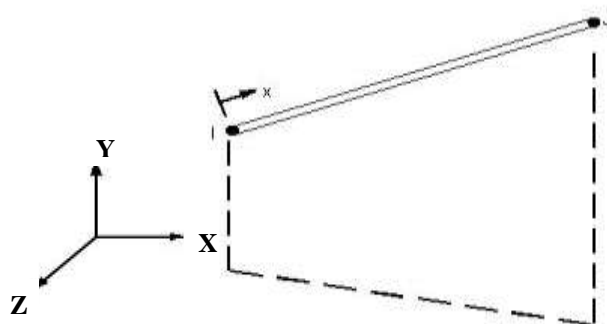


Fig.(7) : Link8 element [10]

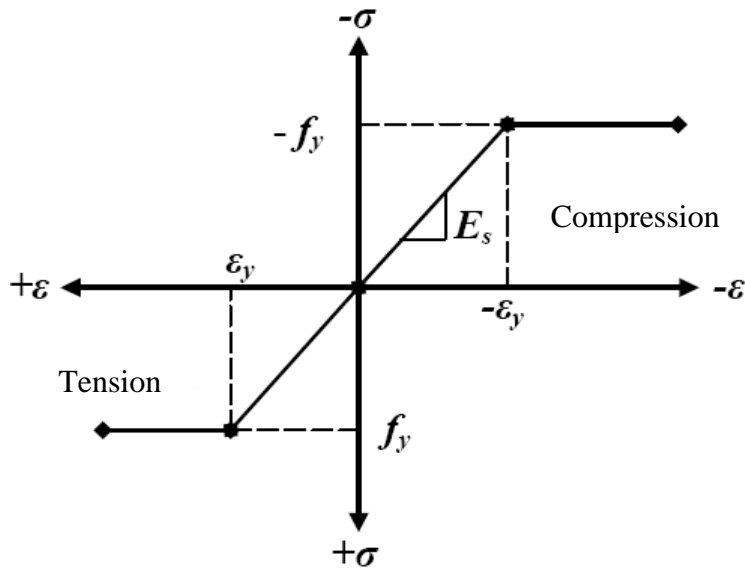


Fig. (8) : Stress-strain curve for steel reinforcement [12]

3.2. Validation of the Finite Element Model :

In order to verify the reliability of the adopted numerical method , including mesh and element type, some of the previous works carried out by other researchers are implemented and reanalyzed and as follows :

3.2.1. Reinforced Concrete Slab with Corner Supports under Static Load:

A square slab of (914.4 mm) side and (44.5 mm) thickness subjected to a central concentrated load was tested by Jorfriet and McNeice in 1971 [13]. This slab was supported at its corners .The slab configuration and material properties are shown in Fig.(9).

Phuvoravan and Sotelino in 2005[14], numerically analyzed this slab using the finite element procedure based on a four node Kirchhoff shell element for concrete with two node Euler beam elements for the steel reinforcing bars. The interaction between reinforcing elements and concrete shell element was achieved by means of rigid links .

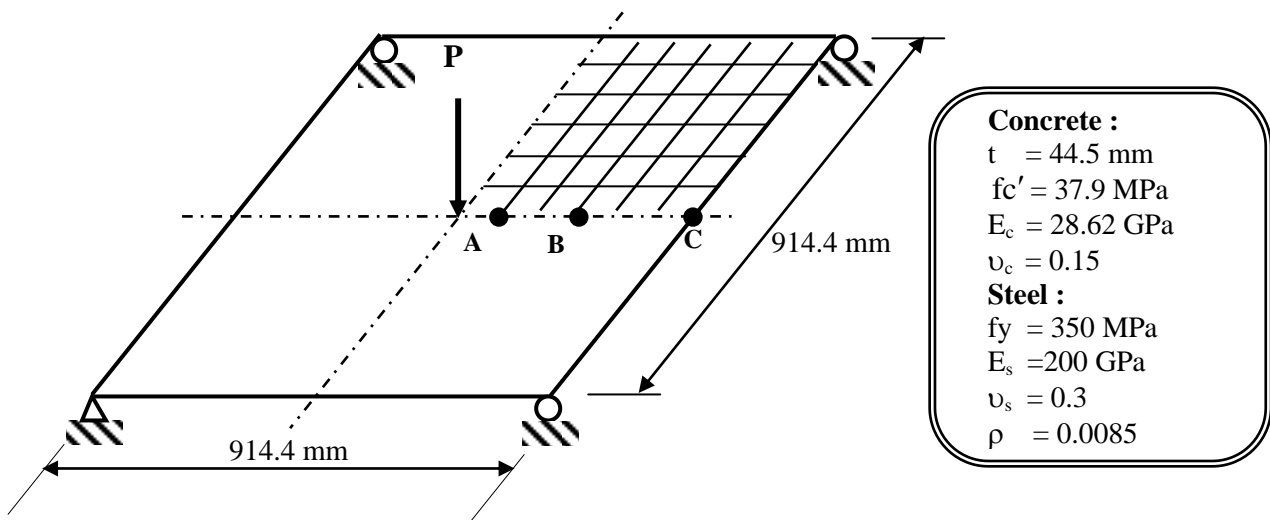


Fig.(9):Schematic of corner-supported reinforced concrete slab tested by Jorfriet and McNeice (1971) [13]

In the present study , the same slab is reanalyzed using 8- noded brick element to model the concrete while two noded link elements are used to model steel reinforcing bars .Using the ANSYS software , (12) elements were chosen in each of the span directions while (3) elements across the thickness of slab were found to give convergent solution .

Figs.(10) and(11) show the finite element idealization which is adopted in the present study .

The nonlinear analysis was performed using a load control technique based on a Newton-Raphson procedure. The number of iterations for the nonlinear solutions was (25) ,while the number of load increments was (50) .

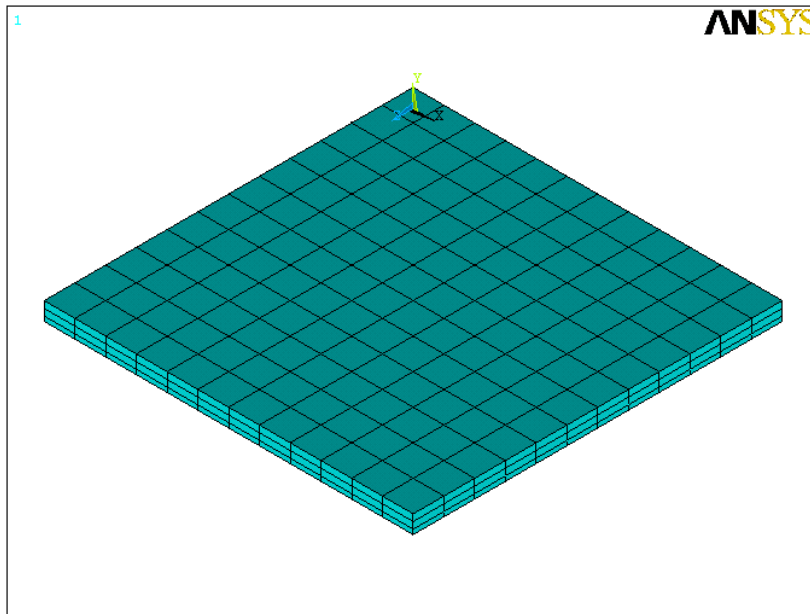


Fig.(10) : Finite element idealization of concrete for the corner –supported slab

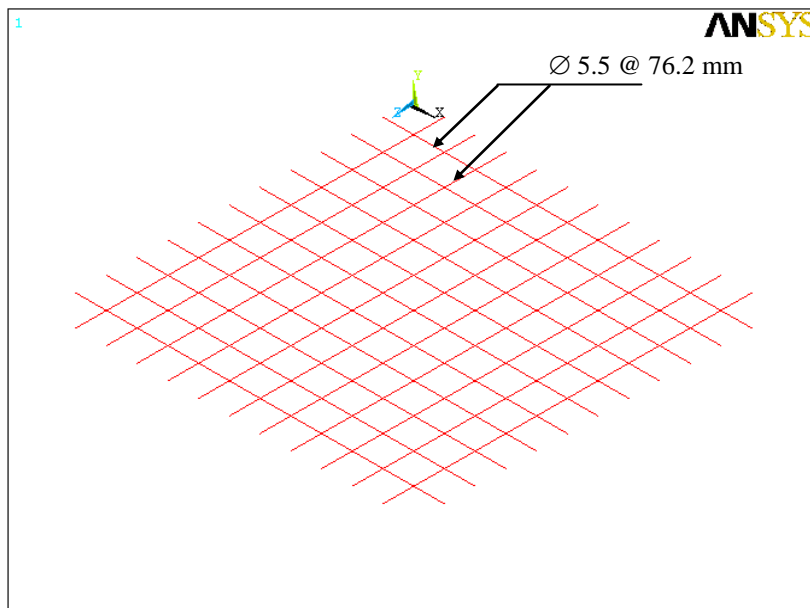


Fig.(11) : Finite element idealization of steel reinforcement for the corner – supported slab

Figs. (12),(13), and (14) show the load-deflection curves of both McNeice experimental results and the numerical finite element results at three points (A , B , and C) on the slab .These point locations are shown at the same plots .

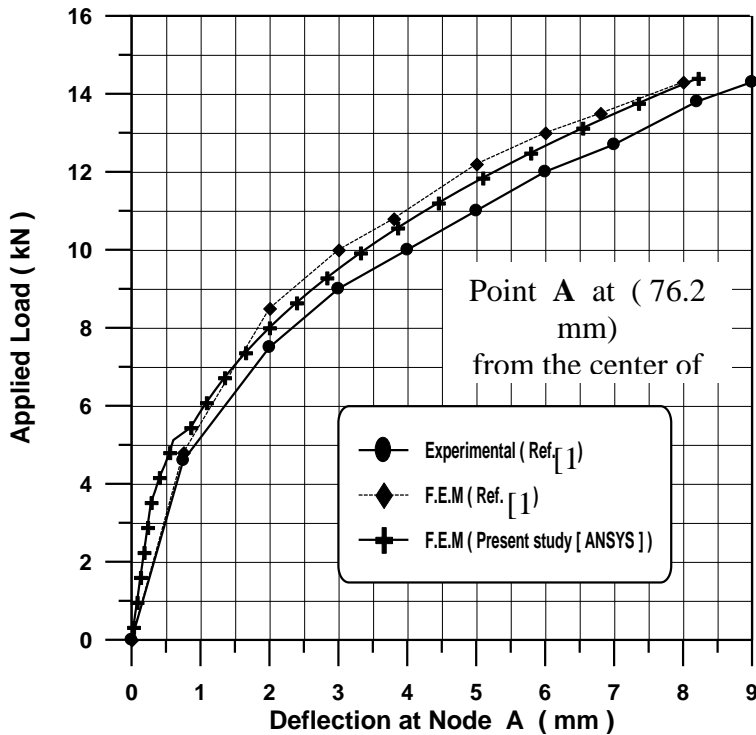


Fig.(12): Load-deflection curves at point (A) of corner – supported slab

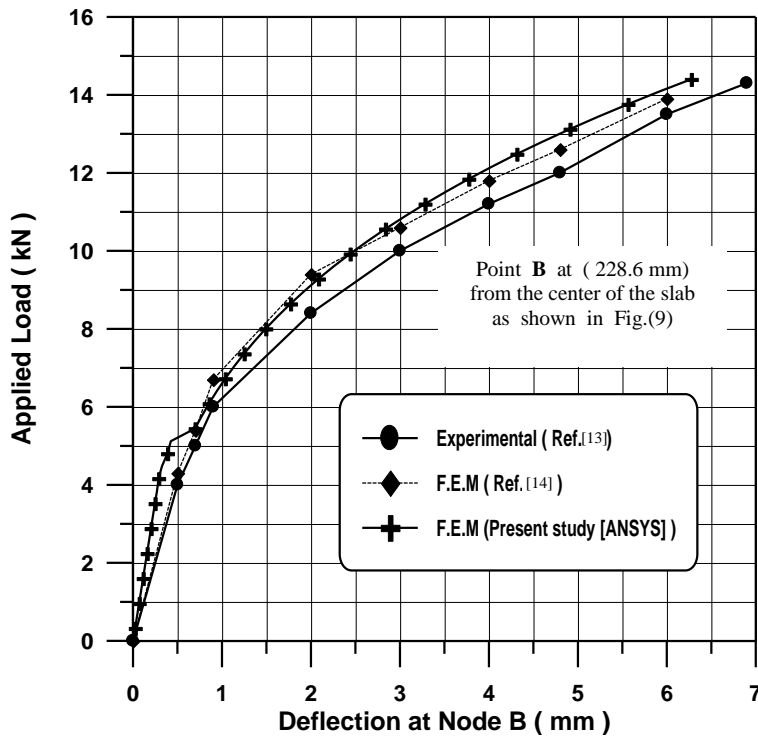


Fig.(13): Load-deflection curves at point (B) of corner – supported slab

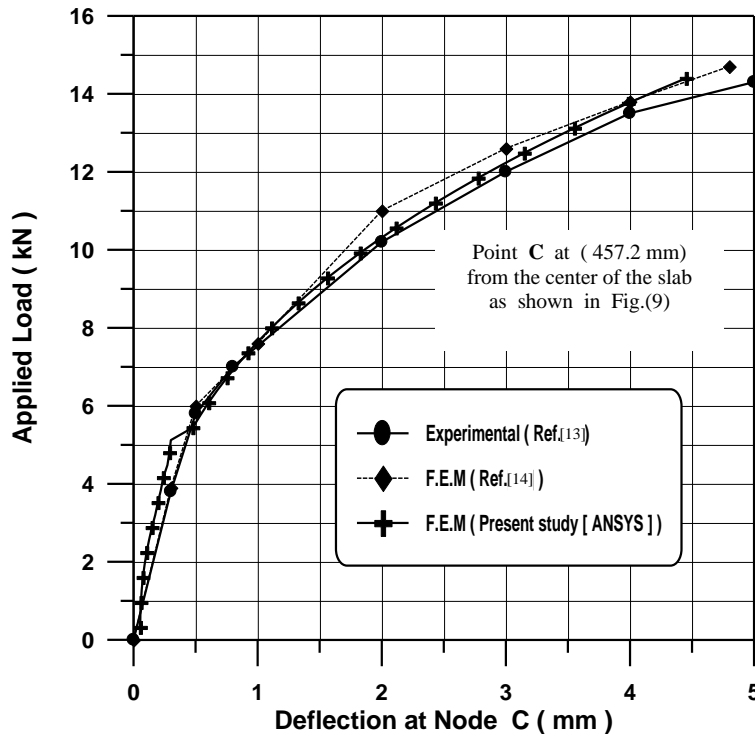


Fig.(14): Load-deflection curves at point (C) of corner – supported slab

3.2.2. A Simply Supported Beam under Stepped Load

A simply supported reinforced concrete beam subjected to two symmetrically applied concentrated loads is analyzed here . The same problem was solved in references [15,16].The geometry, loading and reinforcement of the beam are shown in Figure (15) while material properties are as shown in Table(1)[16].

Ahmed [16] in 2003 , analyzed the beam using the finite element technique based on a degenerated shell element in modeling concrete .Using (20) elements along the span of the beam and six concrete layers in addition to one steel layer across the depth direction .

In the present study , an eight noded brick element is used to model concrete , while two noded link elements are used for the steel reinforcing bars.

Taking advantage of the symmetry in both loading and geometry only one half of the beam is considered. Fig.(16) shows the finite element idealization which is adopted in the present study.

In ANSYS software , the brick elements have an aspect ratio of up to (20) . As this may produce inaccurate results, a simulation with a maximum aspect ratio of (3) was performed for the beam .The model consisted of (540) 8-noded brick elements .

A time step of (0.0005 sec) is considered during the load duration . The number of iterations is (25) .

Fig.(17) shows the dynamic displacement response of the reinforced concrete beam . In this figure , a comparison is made between the nonlinear response obtained by Ahmed[16] with the nonlinear response obtained in the present study. Since both methods are based on acceptable finite element idealization and equal assessment of load increments and factors , the results are shown to be close to each other .

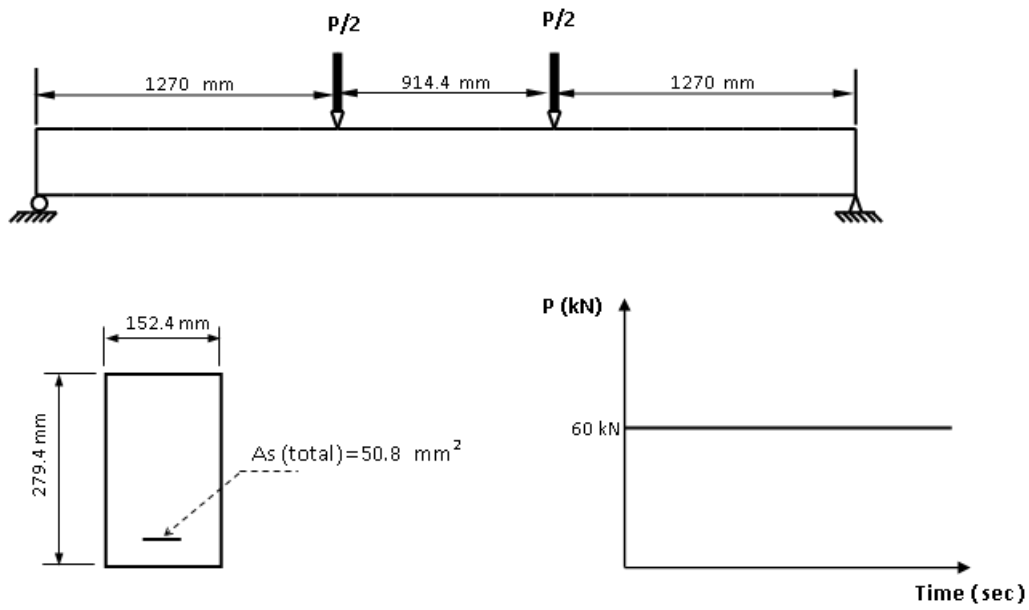


Fig.(15): Geometry ,loading and reinforcement details for reinforced concrete beam under step load

Table(1) Material properties of a simply supported beam[16]

Concrete	
Young's modulus	42055 MPa (6100 ksi)
Ultimate compressive stress	25.78 MPa (3.74 ksi)
Poisson's ratio	0.2
Steel	
Young's modulus	206832 MPa (30000 ksi)
Yield stress	303.35 MPa (44 ksi)
Poisson's ratio	0.3

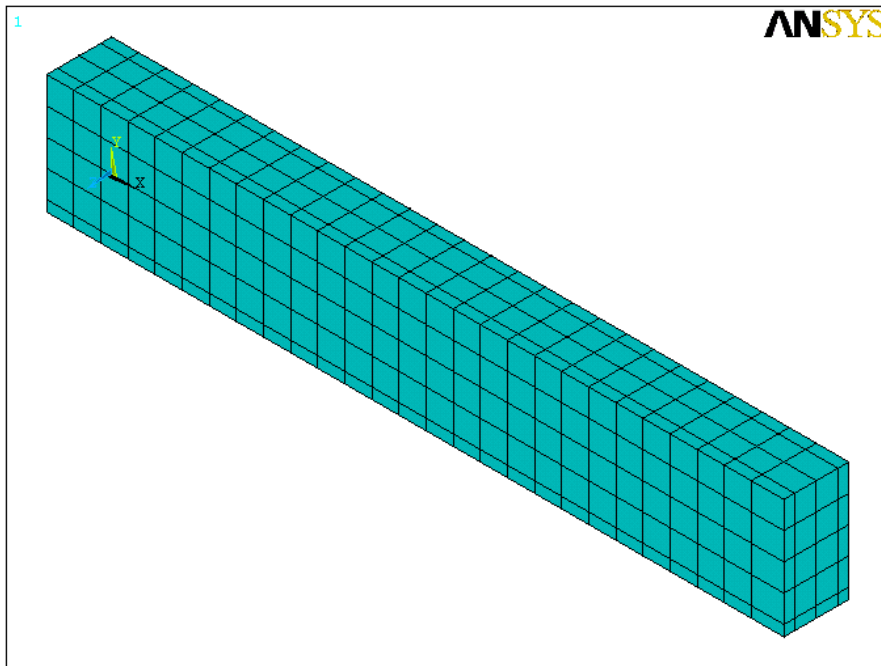


Fig.(16) : Finite element idealization of reinforced concrete beam

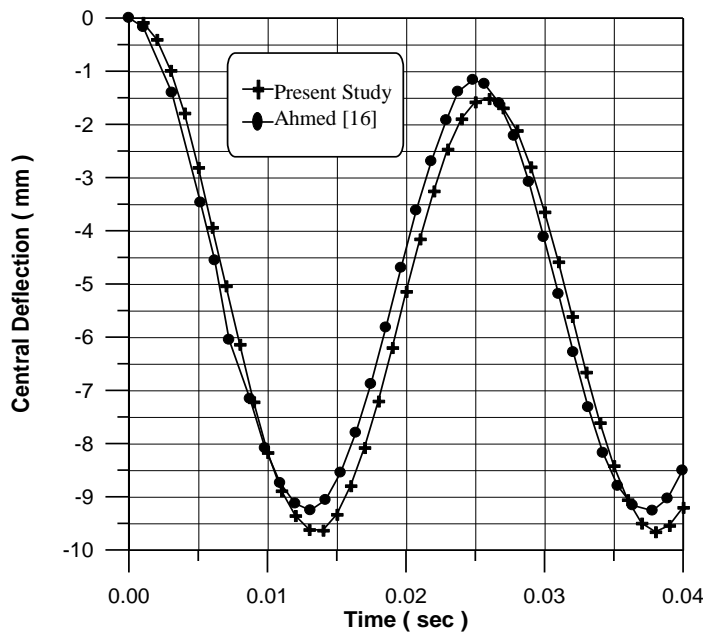


Fig.(17) Nonlinear dynamic response of reinforced concrete beam

4. Reinforced Concrete Slabs under Impact Load :

Some of the slabs tested by Al-Khafaji[7] under impact loads shown in Table (2) were analyzed numerically by the finite element procedure available in the ANSYS software to evaluate both maximum as well as the time history of the deflections .

The actual deflection-time history of the slabs tested by Al-Khafaji[7] under impact loading was not possible to be recorded because of non-availability of sophisticated measuring devices of dynamic deflections, therefore the maximum transient deflections were used for comparison purposes .

Table 2: Details of the slabs tested by Al-Khafaji [7]

Group No.	Slab Dimensions(mm)	Slab No.	Type of Test	Support Condition	Reinf. Ratio %
1	1000x600x50	S11	Static	Simply Supp.	1.18
		D12	Dynamic	Simply Supp.	0.59
		D13	Dynamic	Simply Supp.	1.18
		D14	Dynamic	Clamped	1.18
		D15	Dynamic	Simply Supp.	1.77
2	1000x1000x50	S21	Static	Simply Supp.	1.18
		D22	Dynamic	Simply Supp.	0.59
		D23	Dynamic	Simply Supp.	1.18
		D24	Dynamic	Clamped	1.18
		D25	Dynamic	Simply Supp.	1.77
3	1000x1400x50	S31	Static	Simply Supp.	1.18
		D32	Dynamic	Simply Supp.	0.59
		D33	Dynamic	Simply Supp.	1.18
		D34	Dynamic	Clamped	1.18
		D35	Dynamic	Simply Supp.	1.77

4.1. Slab D12: (Slab dimensions 1000 × 600 × 50 mm ; $\rho = 0.59\%$; simply supported)

The slab is simply supported with a steel reinforcement ratio of (0.59 %) . This slab was tested by Al-Khafaji[7]under an impact load which is caused by a (3 kg) steel ball falling from (1.8 m) height at the center of the slab .

This slab is modeled using (42) brick elements in the long direction , (26) brick elements in the short direction and (3) elements across the thickness while the reinforcing steel was modeled using a total link elements of (580) .The total number of degrees of freedom is (13932) .**Fig.(18)** shows the finite element idealization of slab D12.

For the case of a single impact mass falling from 1.8 m height at the central point of the slab , the load-time history was shown in **Fig.(19)**.

The central deflection –time relation for slab (D12) is given in **Fig.(20)**. It is shown that, the mode of central deflection – time history of the slab is of a sinusoidal shape representing a typical free vibration mode with the exception that the time interval of the rebound is slightly longer than the incidental one .

Accordingly, the stress magnitude in the reinforcing steel also oscillates but , and due to the damping effects , the stress is not in phase with load history (**Fig. (21)**).

The maximum theoretical central deflection of slab D12 that obtained from the present study is (1.43 mm) (for the case of single striking mass falling from 1.8 m) while the experimental test by Al-Khafaji[7] gave a maximum central deflection of (2.93 mm) for the case of repeated impact with increasing height of fall of the striking object up to 1.8 m. This large difference is related to the repetition of strikes in the experimental test which results in accumulated residual deflections.

Finally , crack pattern , as encountered theoretically , almost gave a comprehensive representation of the actual experimental behavior of the tested slab , especially at the lower surface as shown in Fig.(22).

4.2. Slab D13: (Slab dimensions $1000 \times 600 \times 50$ mm ; $\rho = 1.18\%$; simply supported)

The slab is simply supported with a steel reinforcement ratio of (1.18 %) . The finite element mesh is shown in Fig.(23) with a total number of brick elements of (2376) for the slab and (414) link elements for the reinforcing steel which results in a total number of degrees of freedom of (10212) .

The theoretical load-time history of the applied impact load is shown in Fig.(24) . It is shown that the load-time history is not affected noticeably by increasing the reinforcement ratio at the tension zone of the slab.

The theoretical central deflection versus time for the case of a single strike from 1.8 m height of the falling mass , is given in Fig.(25).It is shown that the deflection – time history is also harmonic in nature representing a free vibration mode , however , the time period of the rebound mode dose not differ much in magnitude to that of the incident mode as seen in slab D12 . The reason is that , since slab D13 is with larger steel reinforcement ratio , its stiffness is higher than that of slab D12 and hence the natural frequency is not much sensitive to a slight change of mass caused by the falling steel ball .

The stress-time history in the reinforcing steel is also harmonic in nature and not in phase with the load due to the damping effect (Fig. (26)). The crack patterns of the bottom surface shown in Fig.(27) give a similar distribution as to that of slab D12 in spite of the difference in steel reinforcement ratio.

The maximum theoretical central deflection of slab D13 is (1.01 mm) (for the case of single strike from 1.8 m height of a falling mass)while the experimental test gave a maximum central deflection of (1.69 mm) [7] for the case of repeated impact with increasing height of fall of the striking object up to 1.8 m .

4.3. Slab (D15) : (Slab dimensions $1000 \times 600 \times 50$ mm ; $\rho = 1.77\%$; simply supported)

The slab is simply supported with steel reinforcement ratio of (1.77 %) . The finite element mesh is shown in Fig.(28) with a total number of brick elements of (1512) for the slab and (458) link elements for the reinforcing steel which results in a total number of degrees of freedom of (6612) .

The theoretical load-time history of the applied impact load is shown in Fig.(29) while the central deflection versus time for the case of a single strike from 1.8 m height of a falling mass is given in Fig.(30).It is shown that the deflection – time history is also harmonic in nature representing a free vibration mode , however , the time period of the rebound mode does not differ much in magnitude from that of the incident mode as seen in slab D13 . It is also noticed that increasing the steel reinforcement ratio in slab D15 has insignificant effect on the stiffness of the slab that is, a slight difference between the deflection –time history of slab D15 and slab D13 .

The maximum theoretical central deflection of slab D15 was found to be (0.79 mm) (for the case of a single strike from 1.8 m height of a falling mass)while the experimental test gave a maximum central deflection of (1.01 mm) [7] for the case of repeated impact with increasing height of fall of the striking object up to 1.8 m .

The stress - time history in the reinforcing steel shown in Fig. (31). The crack patterns at the bottom surface of the slab shown in Fig.(32) are of a similar distribution to those of slab D13 in spite of the difference in steel reinforcement ratio.

From Figs.(20,25,30) can be noticed that the theoretical central deflections of the slabs under impact became smaller as the tensile reinforcing steel ratio increases , but the rate of the decrease in the dynamic deflection is less for high steel reinforcement ratio (1.77 %).

4.4. Slab (D14): (Slab dimensions $1000 \times 600 \times 50$ mm ; $\rho = 1.18\%$; **clamped supported**)

This slab is clamped at boundaries with reinforcement ratio of (1.18 %) . The slab was tested by Al-Khafaji[7] under the impact load which is caused by a (3 kg) steel ball falling from 2 m height at the center of the slab .

The finite element mesh for slab D14 is the same as for slab (D13), as shown in Fig.(23).

The theoretical load-time history for a single strike from 2 m height of a falling mass at the central point of the slab is shown in Fig.(33) while the central deflection –time history is shown in Fig.(34). It is shown that the deflection- time history is also of a sinusoidal relation representing a free vibration mode , but this relation is more clear (more oscillation)from that in slab D13 .This tendency is related to the type of supports (clamped supported) . The clamped supports lead to a noticeable increase in stiffness of the slab and hence an increase in the system frequency giving an explicit sinusoidal relation .

Accordingly, the stress magnitude also oscillates more than that of slab D13 as shown in Fig.(35).The maximum theoretical central deflection of slab D14 was found to be (0.336 mm) (for the case of a single strike from 2 m height of a falling mass)while the experimental test gave a maximum central deflection of (1.644 mm) [7] for the case of repeated impact with increasing height of fall of the striking object up to 2 m .This large difference is related to the repetition of strikes with increasing the falling height of the striking object in the experimental test which leads to the development of residual deflections and consequently accumulated deflections .

Crack patterns at the bottom surface that are shown in Fig.(36) reveals the appearance of cracks adjacent to the supports in addition to those developed at the center of the slab .

4.5. SlabD23: (Slab dimensions $1000 \times 1000 \times 50$ mm ; $\rho = 1.18\%$; simply supported)

The slab is simply supported with a steel reinforcement ratio of (1.18 %) . The slab was dimensions of (1000 × 1000 × 50 mm) .The finite element mesh is shown in Fig.(37) with a total number of brick elements of (3888) for the slab and (648) link elements for the reinforcing steel which results in a total number of degrees of freedom of (16428) .

The theoretical load-time history of the applied impact load is shown in Fig.(38) . It is shown that the load-time history is not affected noticeably by increasing the slab dimensions .

The theoretical central deflection versus time for the case of a single strike from 1.8 m height of a falling mass is given in Fig.(39).It is shown that the deflection – time history is also harmonic in nature representing a free vibration mode . It is also found that the deflection-time history is affected slightly by increasing the slab dimensions . This tendency is related to the decrease of the stiffness of the slab due to increasing span of the slab .

The maximum theoretical central deflection of slab D23 is (1.41 mm)(for the case of a single strike from 1.8 m height of a falling mass)while the experimental test gave a maximum central deflection of (2.51 mm) [7] for the case of repeated impact with increasing height of fall of the striking object up to 1.8 m .

The stress - time history in the reinforcing steel shown in Fig. (40).The crack patterns at the bottom surface of the slab shown in Fig.(41)

4.6. Slab (D33) : (Slab dimensions $1000 \times 1400 \times 50$ mm ; $\rho = 1.18\%$; simply supported)

The slab is simply supported with a steel reinforcement ratio of (1.18 %) . The slab was dimensions of $1000 \times 1040 \times 50$ mm .The finite element mesh is shown in Fig.(42) with a total number of brick elements of (5184) for the slab and (864) link elements for the reinforcing steel which results in a total number of degrees of freedom of (21756) .

The theoretical load-time history of the applied impact load is shown in Fig.(43) . The theoretical central deflection versus time for the case of a single strike from 1.8 m height of a falling mass , is given in Fig.(44).It is shown that the deflection – time history is also harmonic in nature representing a free vibration mode . It is also found that the dynamic deflection is increased by increasing the slab dimensions . This tendency is related to the decrease of the stiffness of the slab due to increasing span of the slab .

The maximum theoretical central deflection of slab D33 is (1.66 mm) (for the case of a single strike from 1.8 m height of falling mass)while the experimental test gave a maximum central deflection of (3.16 mm) [7] for the case of repeated impact with increasing height of fall of the striking object up to 1.8 m .

The stress - time history in the reinforcing steel shown in Fig. (45).The crack patterns at the bottom surface of the slab shown in Fig.(46)

From Figs.(25,39,44) can be noticed that the maximum central deflection of the slabs became larger by (20 – 45 %) as the span of the slab increases by (60 – 125 %) .

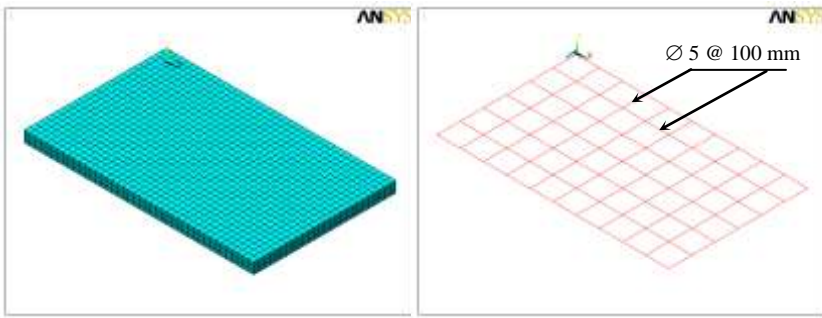
5. CONCLUSIONS :

Based on the theoretical results obtained in the present study , several conclusions may be drawn and can summarized as follows :

1. The theoretical central deflections of the slabs under impact, were found to become smaller when the tensile reinforcing steel ratio increases , but the rate of the decrease in the dynamic deflection is less for high steel reinforcement ratio (1.77 %) , meanwhile , the maximum central deflection of the slabs becomes larger by (20 – 45 %) as the span of the slab increases by (60 – 125 %) .
2. Crack patterns at the bottom surface of the slabs under impact loads were found to be of a similar distribution in all slabs which have the same dimensions in spite of the difference in steel reinforcement ratio.
3. The theoretical load-time history of the applied impact load was not affected noticeably by increasing the reinforcement ratio at the tension zone of the slab .Moreover , the effect of increasing span of the slab on the load-time history was found very little.
4. The mode of the deflection-time history of the slab was found to take a sinusoidal shape representing a typical free vibration mode. Moreover , the stress-time history in the reinforcing steel is harmonic in nature and not in phase with the load due to the damping effect .
5. The deflection-time history for slabs with clamped supports is more oscillatory from that of slabs with simple supported condition . Clamping supports leads to a large increase in the stiffness of the slab and hence, increasing the system frequency with an explicit sinusoidal relation .

REFERENCES:

1. Hughes, G. , and Beeby , A.W. , “Investigation of the Effect of Impact Loading on Concrete Beams”, *Journal of the Structural Engineer* , Vol.60 B , No.3, September 1982.
2. Al-Azzawi, T.K , “ Impact Resistance of Reinforced Concrete Slab”, Ph.D. Thesis , University of Sheffield, England, 1984.
3. Thabit , A. and Haldane, D. , “ Three Dimentional Simulation of Nonlinear Response of Reinforced Concrete Members Subjected to Impact Loading ”, *ACI Structural Journal*, Vol. 97, No. 5, 2000 , pp.689-702.
4. Krutzik, N.J. , “ Analysis of Aircraft Impact Problems”, *Advanced Structural Dynamics* , Applied Science , London , 1980 (as cited by Ahmed (2003)).
5. Al-Azzawi , T.K. and Hussein, A.M. , “ Dynamic Behavior of Reinforced Concrete Model Slabs due to Impact Loading”, *Second Iraqi Conference on Engineering ICE* , 1988.
6. Murtiadi, S. , “ Behavior of High-Strength Concrete Plates under Impact Loading”, M.Sc. Thesis, Faculty of Engineering and Applied Science , Memorial University of Newfoundland, March 1999.
7. Al-Khafaji , A.G. , “ Behavior of Reinforced Concrete Slabs under Impact”, Ph. D. Thesis, Dept. of Civil Eng., College of Eng., University of Baghdad, 2009.
8. Clough, R.W. and Penzien, J. , “ Dynamics of Structures”, *Computers and Structures ,Inc.*, New York ,2003.
9. Chopra, A.K. , “ Dynamics of Structures: Theory and Applications to Earthquake Engineering”, *Prentice Hall* , Englewood Cliffs, New Jersey, 1995.
10. ANSYS 9.0 Inc. , “ ANSYS User’s Manual”, SAS IP , Inc. , Version 9.0, U.S.A., 2004 .
11. Desayi, P. and Krishnan, S.,” Equation for the Stress-Strain Curve of Concrete ”, *ACI Journal* , Vol.61, 1964, pp. 345-350.
12. Kachlakev, D.I. , “ Finite Element Analysis and Model Validation of Shear Deficient Reinforced Concrete Beams Strengthened with GFRP Laminates ”,United States Department of Transportation , Federal Highway Administration , 2001.
13. Jofriet , J.C. and McNeice , G.M. , “Finite Element Analysis of Reinforced Concrete Slabs”, *ASCE Journal of the Structural Division*, Vol.97, No.ST3, March 1971, pp.785 – 805.
14. Phuvoravan , K. and Sotelino, E.D. , “ Nonlinear Finite Element for Reinforced Concrete Slabs”, *ASCE Journal of Structural Engineering*, Vol.131, No.4, April , 2005, pp.643 – 649.
15. Hinton, E. “ Numerical Methods and Software for Dynamic Analysis of Plates and Shells”, *Pineridge Press* , Swansea , 1988 .
16. Ahmed , H.I. , “ Nonlinear Dynamic Analysis of Reinforced Concrete Stiffened Shells using The Finite Element Method”, Ph. D. Thesis, Dept. of Civil Eng., College of Eng., University of Mosul, 2003.



(a) Concrete idealization (b) Steel reinforcement idealization

Fig.(18) : Finite element idealization of slab (D12)

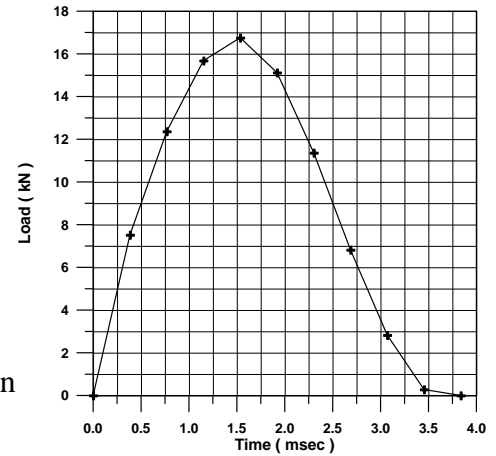


Fig.(19): Load-time history of slab D12

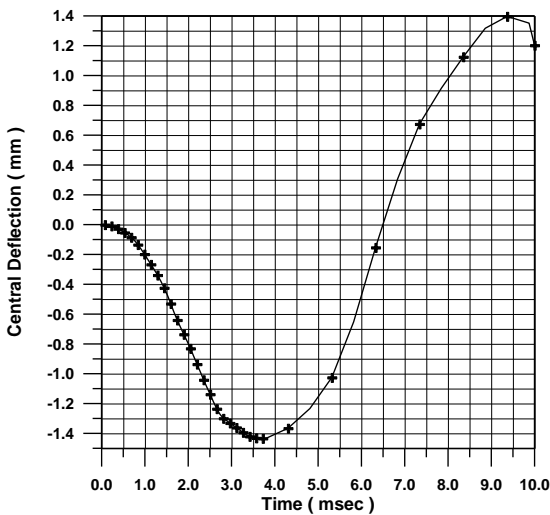


Fig. (20): Theoretical deflection - time curve of slab D12

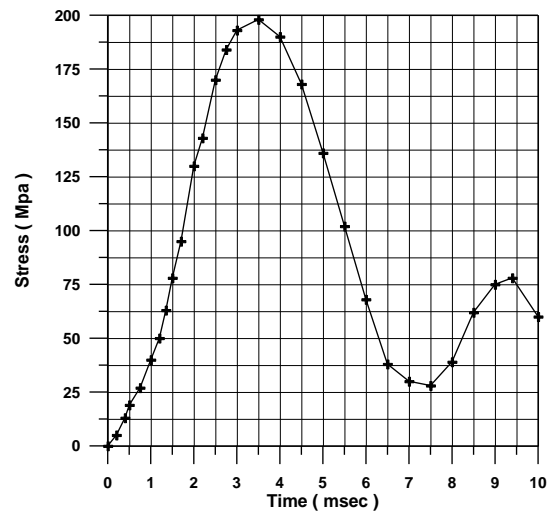


Fig. (21): Stress of steel reinforcement at center of slab D12



(a) At time = 1.534 msec (b) At time = 3.837 msec (c) At time = 10 msec

Fig.(22) : Crack patterns at the bottom face of slab (D12)

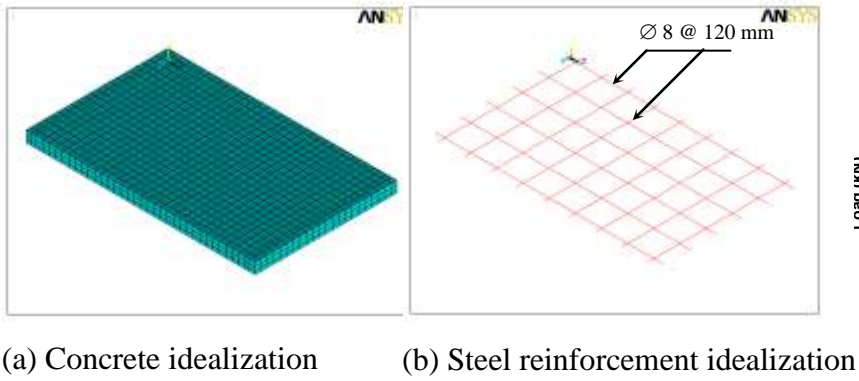


Fig.(23) : Finite element idealization of slab (D13)

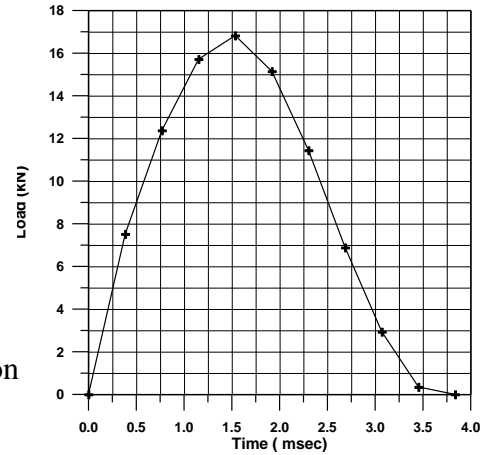


Fig.(24): Load –time history of slab D13

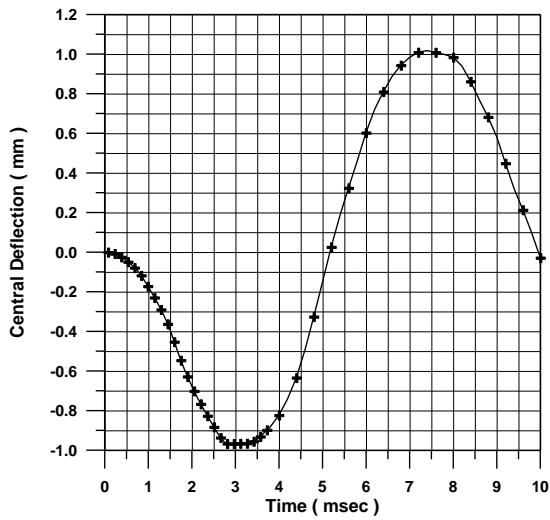


Fig. (25) Theoretical deflection - time curve of slab D13

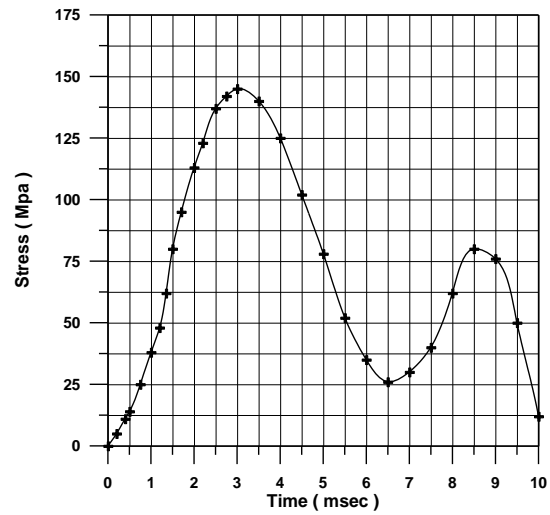
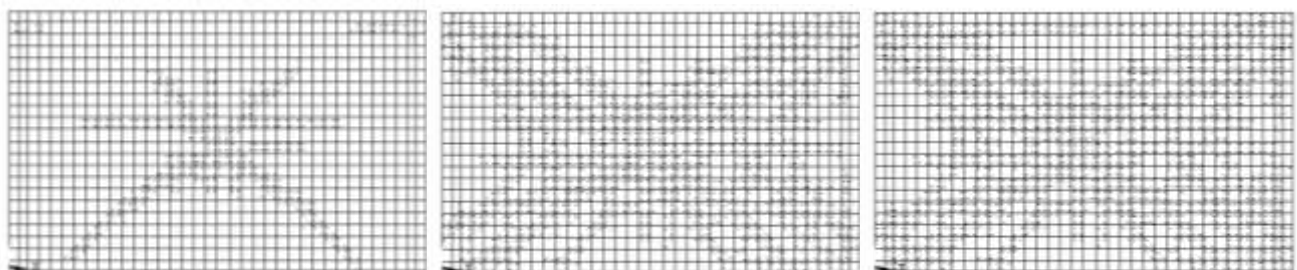
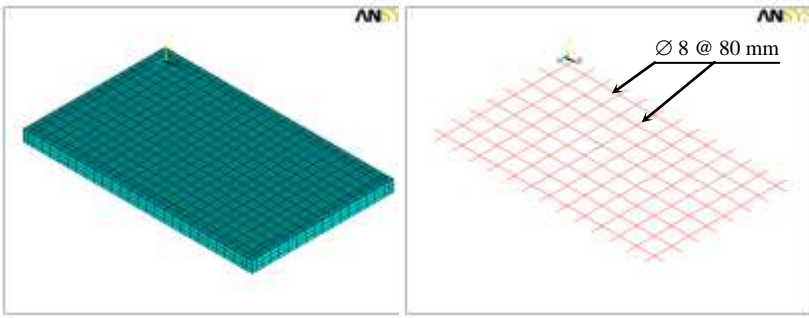


Fig. (26) Stress of steel reinforcement at center of slab D13



(a) At time = 1.534 msec (b) At time = 3.837 msec (c) At time = 10 msec

Fig.(27) : Crack patterns at the bottom face of slab (D13)



(a) Concrete idealization (b) Steel reinforcement idealization

Fig.(28) : Finite element idealization of slab (D15)

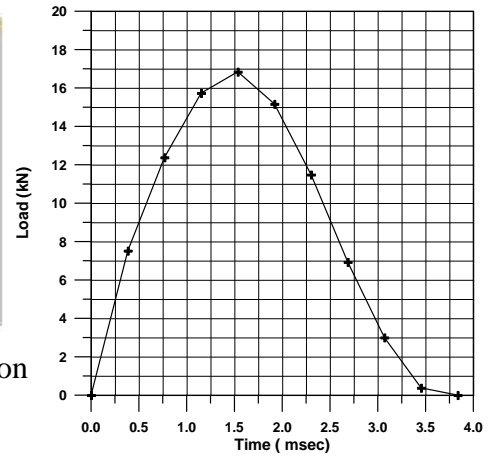


Fig.(29): Load –time history of slab D15

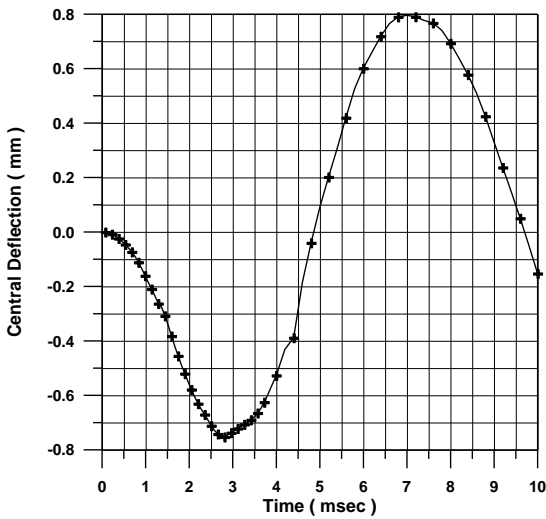


Fig. (30) Theoretical deflection - time curve of slab D15

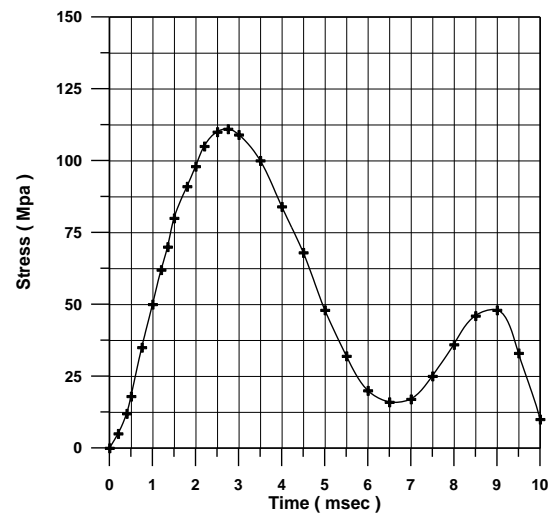
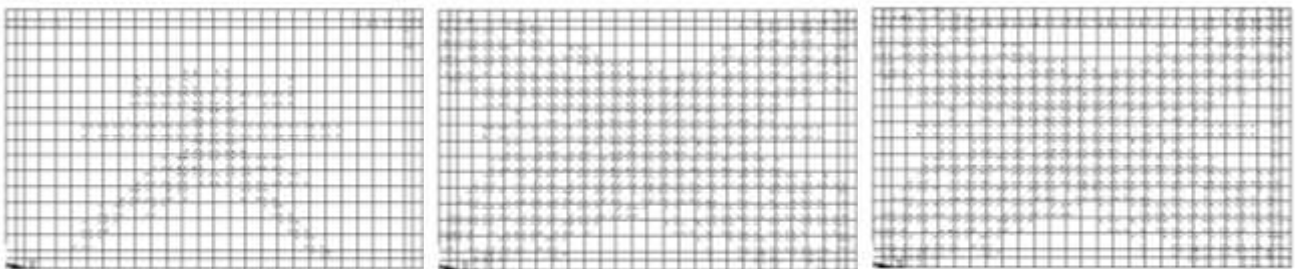


Fig. (31) Stress of steel reinforcement at center of slab D15



(a) At time = 1.534 msec (b) At time = 3.837 msec (c) At time = 10 msec

Fig.(32) : Crack patterns at the bottom face of slab (D15)

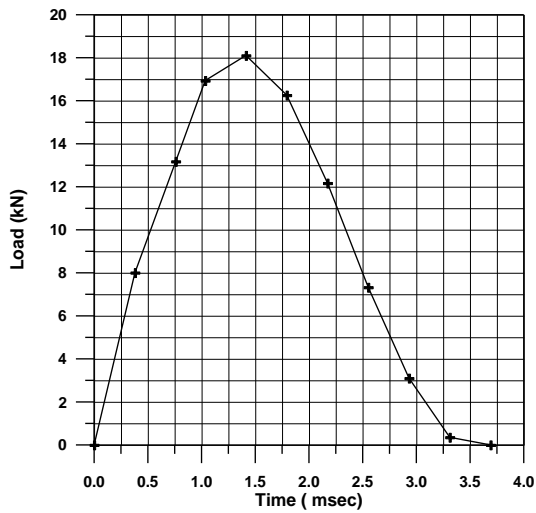


Fig.(33): Load –time history of slab D14

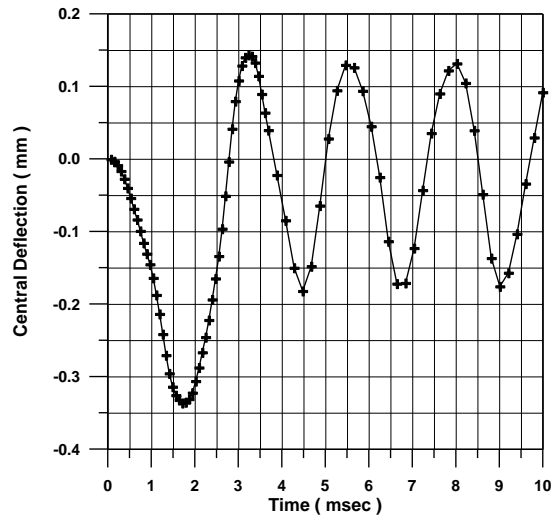


Fig. (34) Theoretical deflection - time curve of slab D14

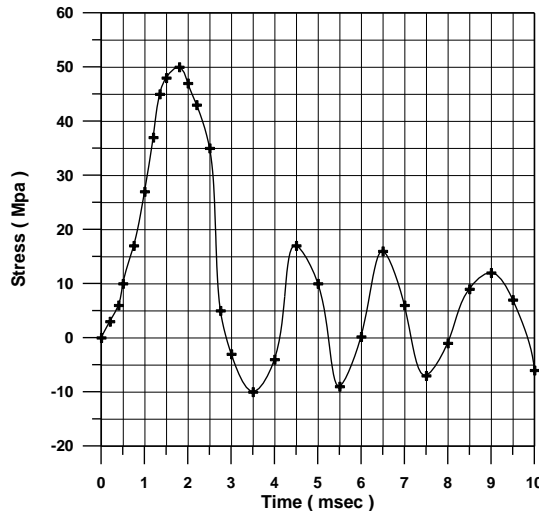


Fig. (35) Stress of steel reinforcement at center of slab D14

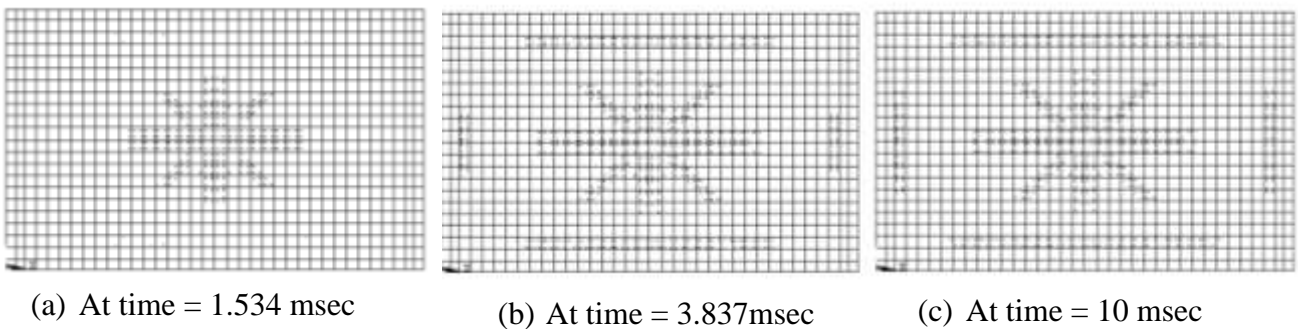
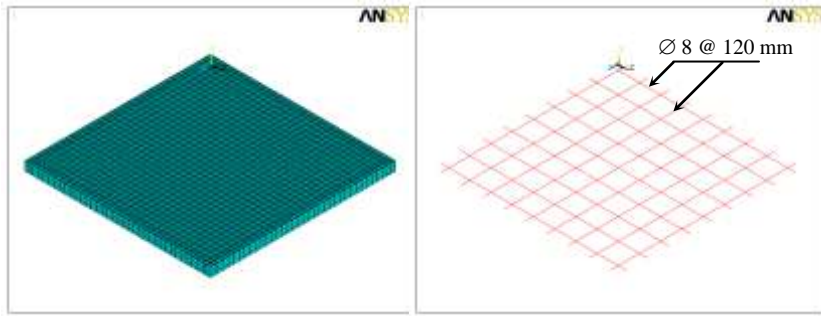


Fig.(36) : Crack patterns at the bottom face of slab (D14)



(a) Concrete idealization (b) Steel reinforcement idealization

Fig.(37) : Finite element idealization of slab (D23)

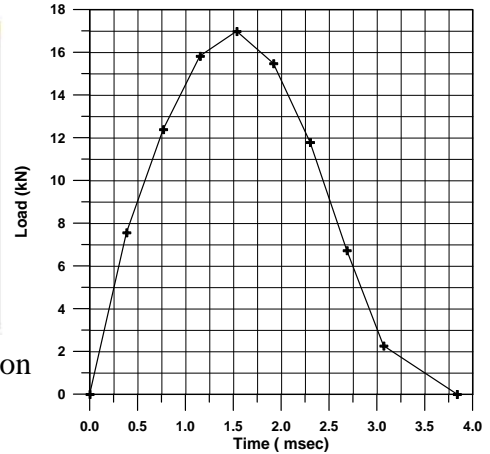


Fig.(38): Load –time history of slab D23

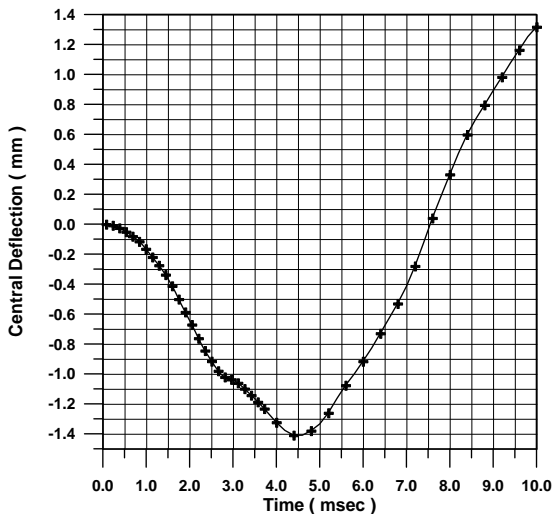


Fig. (39) Theoretical deflection - time curve of slab D23

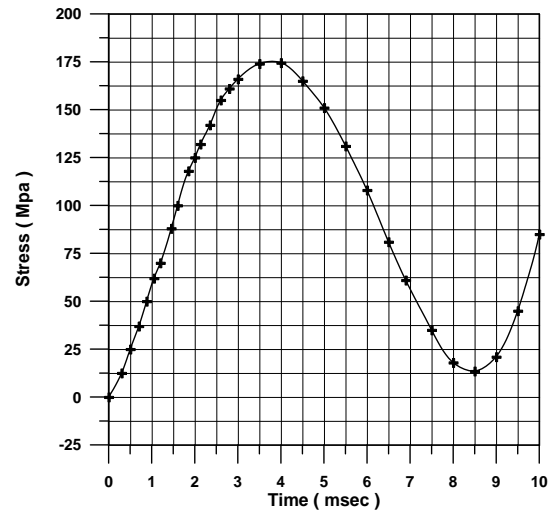
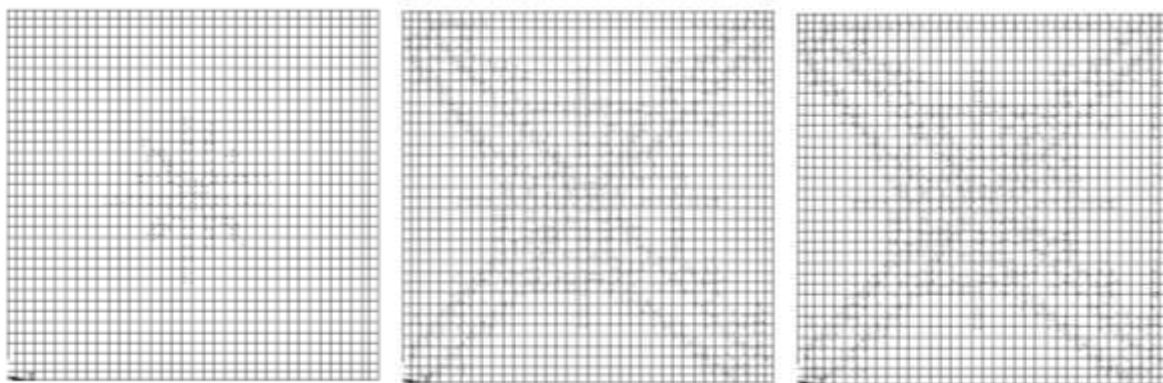
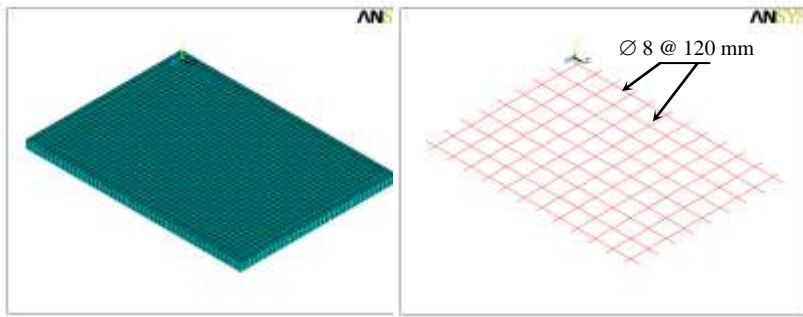


Fig. (40) Stress of steel reinforcement at center of slab D23



(a) At time = 1.534 msec (c) At time = 3.837 msec (b) At time = 10 msec

Fig.(41) : Crack patterns at the bottom face of slab (D23)



(a) Concrete idealization (b) Steel reinforcement idealization

Fig.(42) : Finite element idealization of slab (D33)

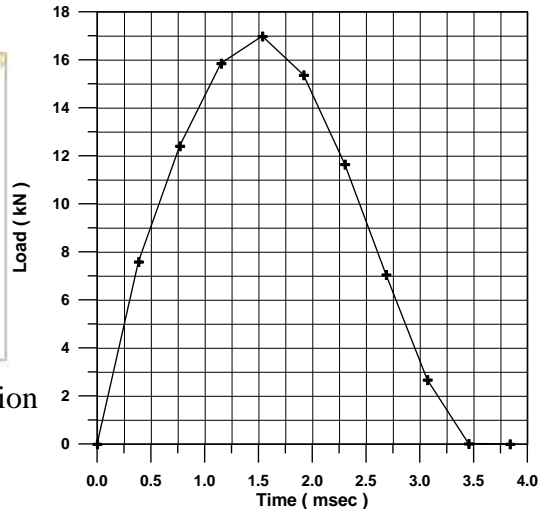


Fig.(43): Load –time history of slab D33

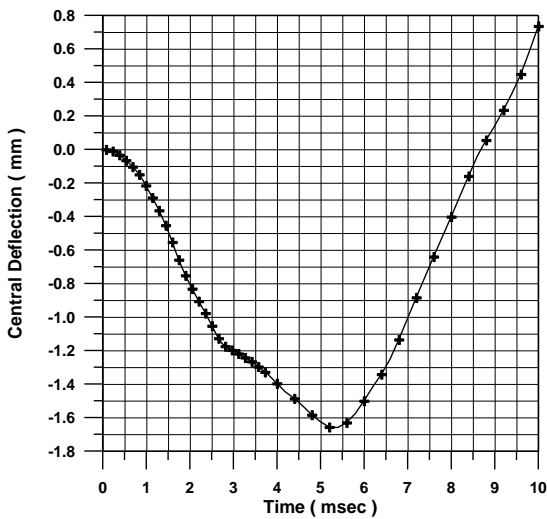


Fig. (44) Theoretical deflection - time curve of slab D33

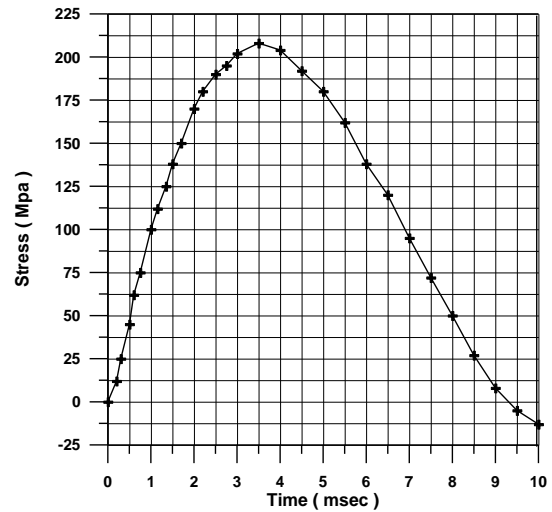


Fig. (45) Stress of steel reinforcement at center of slab D33



(a) At time = 1.534 msec (b) At time = 3.837 msec (c) At time = 10 msec

Fig.(46) : Crack patterns at the bottom face of slab (D33)